BULLETIN OF THE EARTHQUAKE
RESEARCH INSTITUTE
Vol. 41 (1963), pp. 61-81

6. *Directivity of Tsunamis.*

By Tokutaro HATORI,

Earthquake Research Institute.

(Read Nov. 27, 1962.—Received Dec. 28, 1962.)

1. Introduction

On the problem of directivity of tsunami, T. Matuzawa[1], S. Yamaguti[2], Z. Suzuki et al[3], and H. Miyoshi[4] discussed the cases of the 1933 Sanriku tsunami and the one off Tokachi in 1952. On the other hand, N. Miyabe[5] and S. Omote[6] have shown that the generating area of a tsunami should be considered a broad area. K. Iida[7] obtained a relation between the linear dimension of a tsunami domain and the earthquake magnitude, and has suggested the identity of the origin area of tsunami and the after-shock area. Also, T. Hirono[8] has suggested that the epicenter of main-shock is at a corner of the origin area of tsunami.

Recent investigations of after-shocks and the propagation of tsunami waves have revealed the fact that most of the tsunami generating areas seem to be strongly elliptic in shape. T. Momoi[9][10][11] discussed theoreti-

1) T. MATUZAWA, "Directivity of Tsunami," *Journ. Seismol. Soc. Japan*, [i], **9** (1937), 23, (in Japanese).

2) S. YAMAGUTI, "Abnormally High Waves or Tsunami, on the Coast of Sanriku in Japan, on March 3, 1933," *Bull. Earthq. Res. Inst., Suppl. Vol.*, **1** (1934), 36.

3) Z. SUZUKI, K. NORITOMI, J. OSSAKA and A. TAKAGI, "On the Tsunami in Sanriku District accompanying the Tokachi Earthquake, March 4, 1952," *Sci. Rep. Tohoku Univ., Geophysics* [V], **4** (1953), 134.

4) H. MIYOSHI, "Directivity of the Recent Tsunamis," *Journ. Oceanogr. Soc. Japan*, **11** (1955), 151.

5) N. MIYABE, "An Investigation of the Sanriku Tsunami based on Mareogram Data," *Bull. Earthq. Res. Inst., Suppl., Vol.*, **1** (1934), 112.

6) S. OMOTE, "On the Central Area of Seismic Sea Waves," *Bull. Earthq. Res. Inst.*, **25** (1947), 15.

7) K. IIDA, "Magnitude and Energy of Earthquakes accompanied by Tsunami, and Tsunami Energy," *Journ. Earth Sci., Nagoya Univ.*, **6** (1958), 101.

8) T. HIRONO, The Dictionary of Oceanography, Tokyo-do Co., (1960), 272, (in Japanese).

9) T. MOMOI, "On the Directivity of Water Waves Generated by a Vibrating Elliptic Wave Source," *Bull. Earthq. Res. Inst.*, **40** (1962), 287.

10) T. MOMOI, "The Directivity of Tsunami (1) The Case of Instantaneously and Uniformly Elevated Elliptic Wave Origin," *Bull. Earthq. Res. Inst.*, **40** (1962), 297.

11) T. MOMOI, "Some Remarks on Generation of Waves from Elliptical Wave Origin," *Bull. Earthq. Res. Inst.*, **41** (1963), 1.

Table 1. List of tsunamis. L: A linear dimension of tsunami domain. a: Length of the major axis of an after-shock area, b: Length of the minor axis of an after-shock area.

No.	Date	Epicenter Latitude N	Epicenter Longitude E	Location	M	L km	a km	b/a
1	Mar. 3, 1933	39.1	144.7	Sanriku	8.3	600	280	0.65
2	Oct. 13, 1935	40.0	143.6	Off Miyako	7.2	100	75	0.78
3	May 23, 1938	36.7	141.4	Off Shioya	7.1	90	120	0.68
4	Nov. 5, 1938	37.1	141.65	Off Fukushima	7.7	120	120	0.73
5	Dec. 7, 1944	33.7	136.2	Tonankai	8.0	200	160	0.36
6	Mar. 4, 1952	42.15	143.85	Off Tokachi	8.1	120	200	0.54
7	Nov. 4, 1952	52	162	Kamchatka	8.2		830	0.34
8	Nov. 26, 1953	34.3	141.8	Off Bōsō	7.5		100	0.39
9	Nov. 7, 1958	44.0	148.7	Iturup	8.0		190	0.71
10	May 24, 1960	38 S	73.5 W	Chile	8.4		880	0.23
11	Feb. 27, 1961	31.6	131.85	Hiuganada	7.2	80	70	0.52
12	Mar. 9, 1931	41.2	142.5	Off Hachinohe	7.6	50	70	0.68
13	Nov. 2, 1931	32.2	132.1	Hiuganada	6.6		40	0.54
14	Oct. 18, 1935	40.3	144.2	Off Miyako	7.1		50	0.64
15	Nov. 3, 1936	38.2	142.2	Off Kinkazan	7.7	90	80	0.65
16	May 1, 1939	39.95	139.8	Oga Pen.	6.7	40	40	0.67
17	Nov. 19, 1941	32.6	132.1	Hiuganada	7.4		50	0.50
18	Jun. 13, 1934	41.1	142.7	Off Hachinohe	7.1		90	0.58
19	Jan. 13, 1945	34.7	137.2	Mikawa Bay	7.1		50	0.69
20	Feb. 10, 1945	40.9	142.1	Off Hachinohe	7.3		150	0.53
21	Dec. 21, 1946	33.0	135.6	Nankaido	8.1	350		
22	Nov. 4, 1947	43.8	141.0	Off Rumoe	7.0		80	0.65

cally some problems of tsunami generation from an elliptic origin. R. Takahasi and T. Hatori[12] carried out a model experiment on the tsunami generation from an elliptic origin.

In this paper, it is assumed that tsunami waves are generated from the after-shock area. Directivities of wave-height, period and energy are examined for 11 tsunamis that occurred off the coasts of Japan, Iturup, Kamchatka and Chile as shown in Table 1.

12) R. TAKAHASI and T. HATORI, "A Model Experiment on the Tsunami Generation from a Bottom Deformation Area of Elliptic Shape," *Bull. Earthq. Res. Inst.*, **40** (1962), 873, (in Japanese).

2. The relation between the generating area of tsunami and the after-shock area

As to the tsunamis which occurred in the adjacent sea of Japan, the linear dimension of the tsunami domain L, obtained with the aid of the inverse refraction diagram is roughly proportional to the domain of an after-shock a as shown in Fig. 1 except for the 1933 Sanriku tsunami.

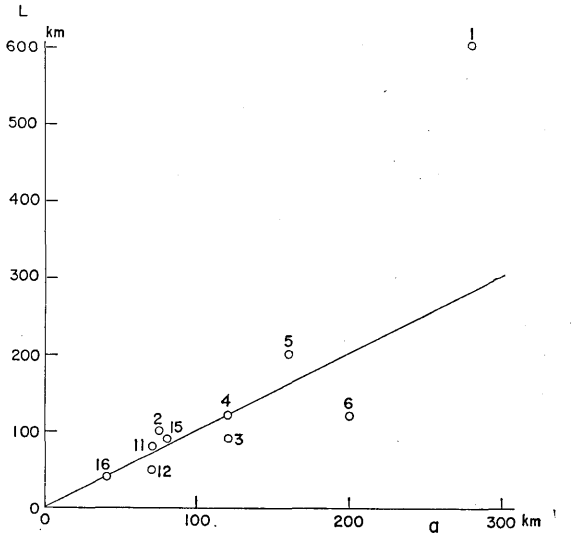

Fig. 1. The relation between a and L. a: Length of the major axis of an after-shock area. L: A linear dimension of tsunami domain.

However, these relationships involve many problems when the linear dimension of an after-shock area is much larger than, say, 900 Km, or the after-shocks are distributed widely on land. The 1952 Kamchatka earthquake and the 1960 Chilean earthquake are examples of the former case and the 1923 Kanto earthquake and the 1946 Nankaido earthquake are examples of the latter.

3. Form of the after-shock area

The so-called after-shock area which covers the epicenters of after-shocks seems to be roughly elliptic in shape, although the precision is limited by the accuracy of observation. T. Utsu and A. Seki[13] obtained

13) T. UTSU and A. SEKI, "A Relation between the Area of After-shock Region and the Energy of Main-shock," *Journ. Seismol. Soc. Japan*, [ii], **7** (1955), 233, (in Japanese).

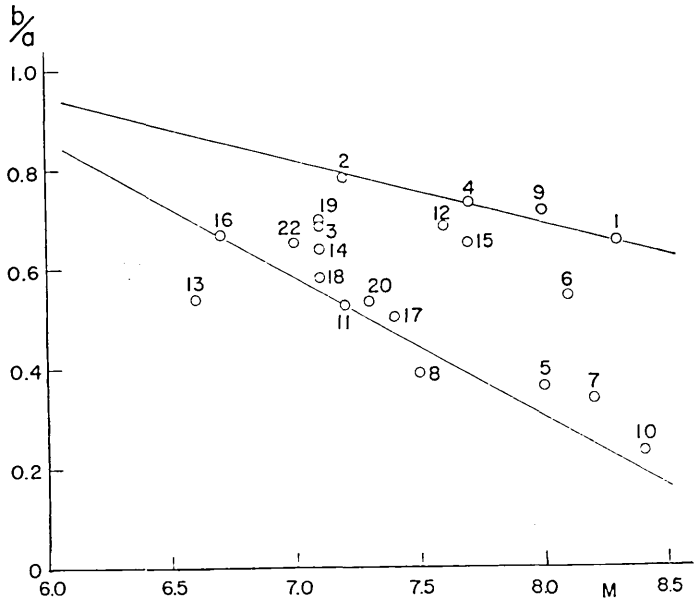

Fig. 2. The relation between ratio of elliptic axes of an after-shock area and earthquake magnitude.

a relation between the after-shock area and the earthquake magnitude.

The after-shock areas of tsunami-generating earthquakes, assumed to be elliptic in shape, are shown in Table 1, where a and b denote the major and the minor axes of the after-shock area. As shown in Fig. 2 we find that in general the relationship between axis ratio of ellipse b/a and the earthquake magnitude is

$$b/a = AM + B \,.$$

Numerical values of the constants A and B obtained graphically are

$$A = -(0.13 \sim 0.28), \quad B = 1.69 \sim 2.56 \,.$$

The after-shock area appears to become strongly elliptical when the earthquake magnitude increases. R. Takahasi and T. Hatori[14] found a relation between the after-shock area and the linear dimension of tsunami domain, provided that the origin area of tsunami is assumed to be equal to the after-shock area. For $b/a=1$, the earthquake magnitude becomes 5.5 from the above equation. K. Iida[7] noticed that the earthquake magnitude 6.4 is the limiting magnitude below which tsunami does not occur as far as the Japanese data is concerned. In this case the shape

of the after-shock area will be roughly circular.

4. Wave-height

The area of after-shock corresponds approximately to that of crustal deformation. The original area of a tsunami corresponds to the area of crustal deformation. Thus, tsunami waves must be generated from an after-shock area. The distributions of wave-heights near the coast of tsunami origin are examined for 11 tsunamis.[15) to 31)] The data of the after-shock has been extracted from the reports of the Japan Meteorological Agency, and U. S. Coast and Geodetic Survey. Figs. 3 to 13

14) R. TAKAHASI and T. HATORI, "On the Tsunami which accompanied the Hiuganada Earthquake of Feb. 27, 1961," *Bull. Earthq. Res. Inst.*, **39** (1961), 561, (in Japanese).

15) *Bull. Earthq. Res. Inst., Suppl. Vol.*, **1** (1934).

16) K. IIDA, "Earthquakes accompanied by Tsunamis occurring under the Sea off the Island of Japan," *Journ. Earth Sci., Nagoya Univ.*, **4** (1956), 1.

17) S. OMOTE, "The Tsunami, the Earthquake Sea Waves, that accompanied the Great Earthquake of Dec. 7, 1944," *Bull. Earthq. Res. Inst.*, **24** (1946), 31, (in Japanese).

18) CENTRAL METEOROLOGICAL OBSERVATORY, "Report on the Tonankai Earthquake of December 7, 1944," *Quart. Journ. Seismol.*, (1945), 1, (in Japanese).

19) CENTRAL METEOROLOGICAL OBSERVATORY, "The Tokachi Earthquake of March 4, 1952," *Quart. Journ. Seismol.*, **17** (1953), 1, (in Japanese).

20) Z. SUZUKI and K. NAKAMURA, "On the Heights of the Tsunami on March 4, 1952, in the District near Erimo-misaki," *Sci. Rep. Tohoku Univ.*, Geophysics [v] **4** (1953), 139.

21) Бюллетень Совета по Сейсмологии No. 4 Цунами 4-5 Ноября 1952 Г., Издательство Акад. Наук СССР, Москва, (1958).

22) CENTRAL METEOROLOGICAL OBSERVATORY, "Report of the Investigation on the Kamchatka Earthquake," *Quart. Journ. Seismol.*, **18** (1953), 1, (in Japanese).

23) CENTRAL METEOROLOGICAL OBSERVATORY, "The Bōsō-oki Earthquake of November 26, 1953," *Quart. Journ. Seismol.*, **19** (1954), 42, (in Japanese).

24) S. L. SOLOV'EV and M. D. FERCHEV, "Summary of Data on Tsunami in the USSR," *Bull. Coun. Seismol. Acad. Sci. USSR*, **9** (1961), 23.

25) THE JAPAN METEOROLOGICAL AGENCY, "The Etorofu-oki Earthquake of November 7, 1958," *Quart. Journ. Seismol.*, **24** (1959), 65, (in Japanese).

26) J. M. SYMONS and B. D. ZETLER, "The Tsunami of May 22, 1960 as Recorded at Tide Stations, Preliminary Rep.," *U. S. Department Commerce, C. G. S.*, (1960).

27) T. HAGIWARA and I. KAYANO, "Seismological Data of Chilean Earthquakes in 1960," *Rep. Chilean Tsunami, Field Invest. Comm. Chilean Tsunami* (1961), 35.

28) K. HORIKAWA, "Outline of the Tsunami of 1960 in Chile and Other Places," *Kaigan*, **28** (1961), 1, (in Japanese).

29) R. TAKAHASI and T. HATORI, "A Summary Report on the Chilean Tsunami of May 1960," *Rep. Chilean Tsunami, Field Invest. Comm. Chilean Tsunami* (1961), 23.

30) JAPAN METEOROLOGICAL AGENCY, "The Report on the Tsunami of the Chilean Earthquake, 1960," *Techn. Rep. Japan Meteor. Agen.*, **8** (1961), 1, (in Japanese).

31) JAPAN METEOROLOGICAL AGENCY, "The Hyuganada Earthquake of Feb. 27, 1961," *Quart. Journ. Seismol.*, **26** (1961), 81, (in Japanese).

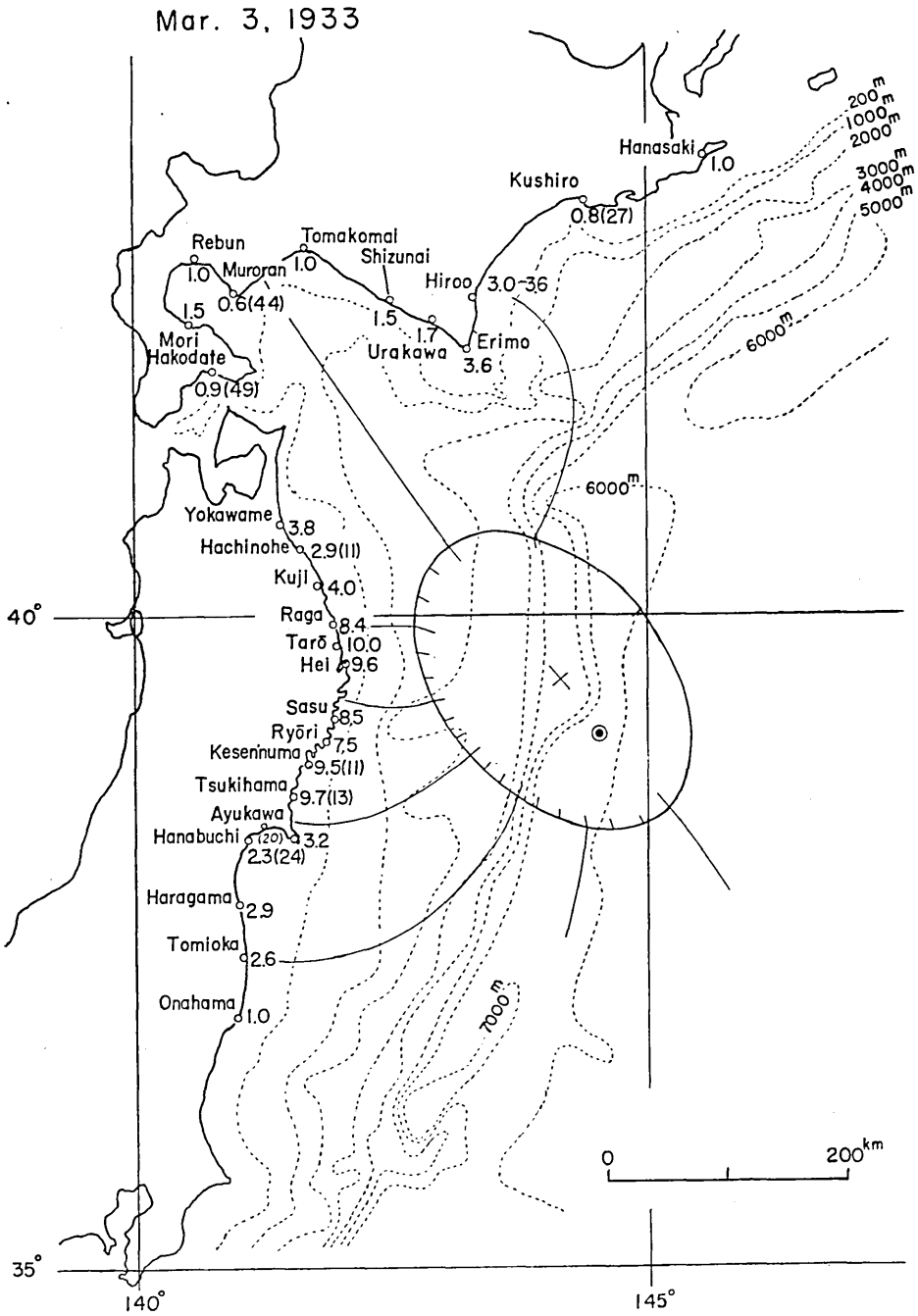

Fig. 3. The after-shock area, the distribution of inundation heights in m and periods in min, for the tsunami of Mar. 3, 1933.

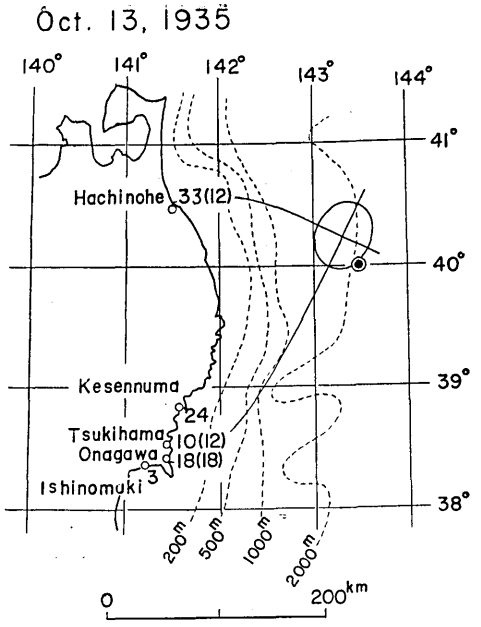

Fig. 4. The after-shock area, the distribution of wave-heights in cm and periods in min, for the tsunami of Oct. 13, 1935.

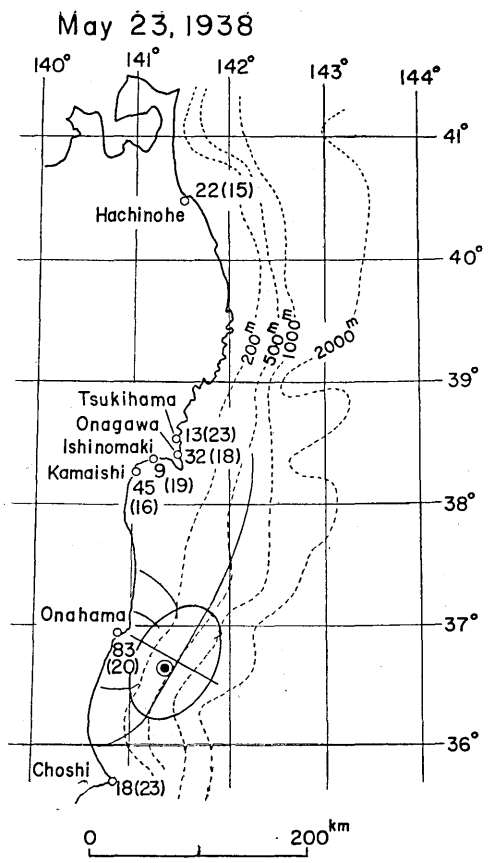

Fig. 5. The after-shock area, the distribution of wave-heights in cm and periods in min, for the tsunami of May 23, 1938.

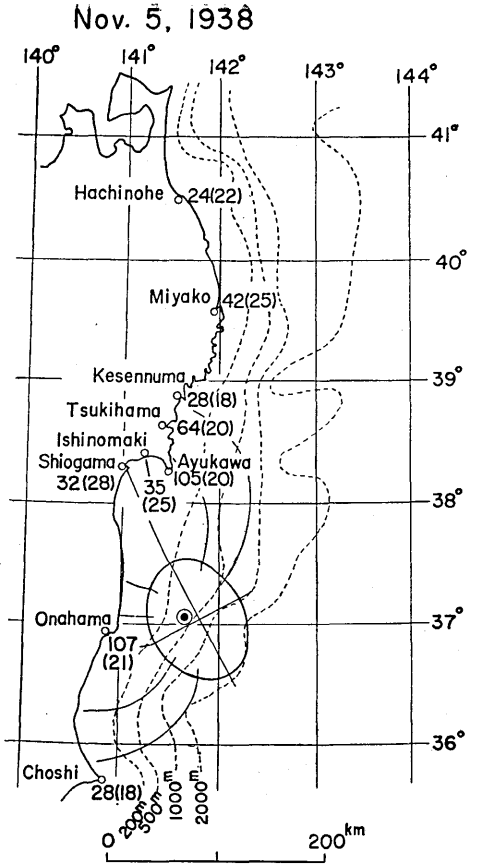

Fig. 6. The after-shock area, the distribution of wave-heights in cm and periods in min, for the tsunami of Nov. 5, 1938.

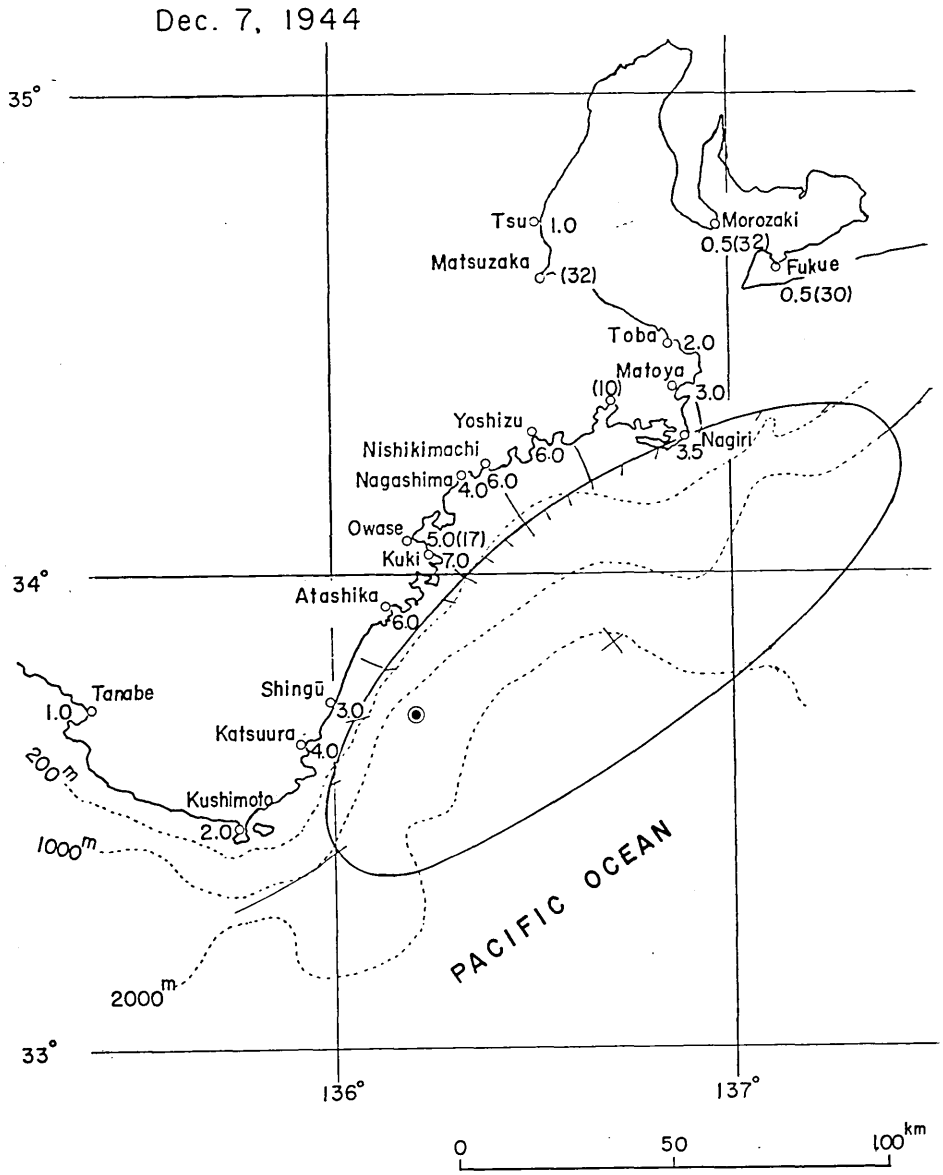

Fig. 7. The after-shock area, the distribution of inundation heights in m and periods in min, for the tsunami of Dec. 7, 1944.

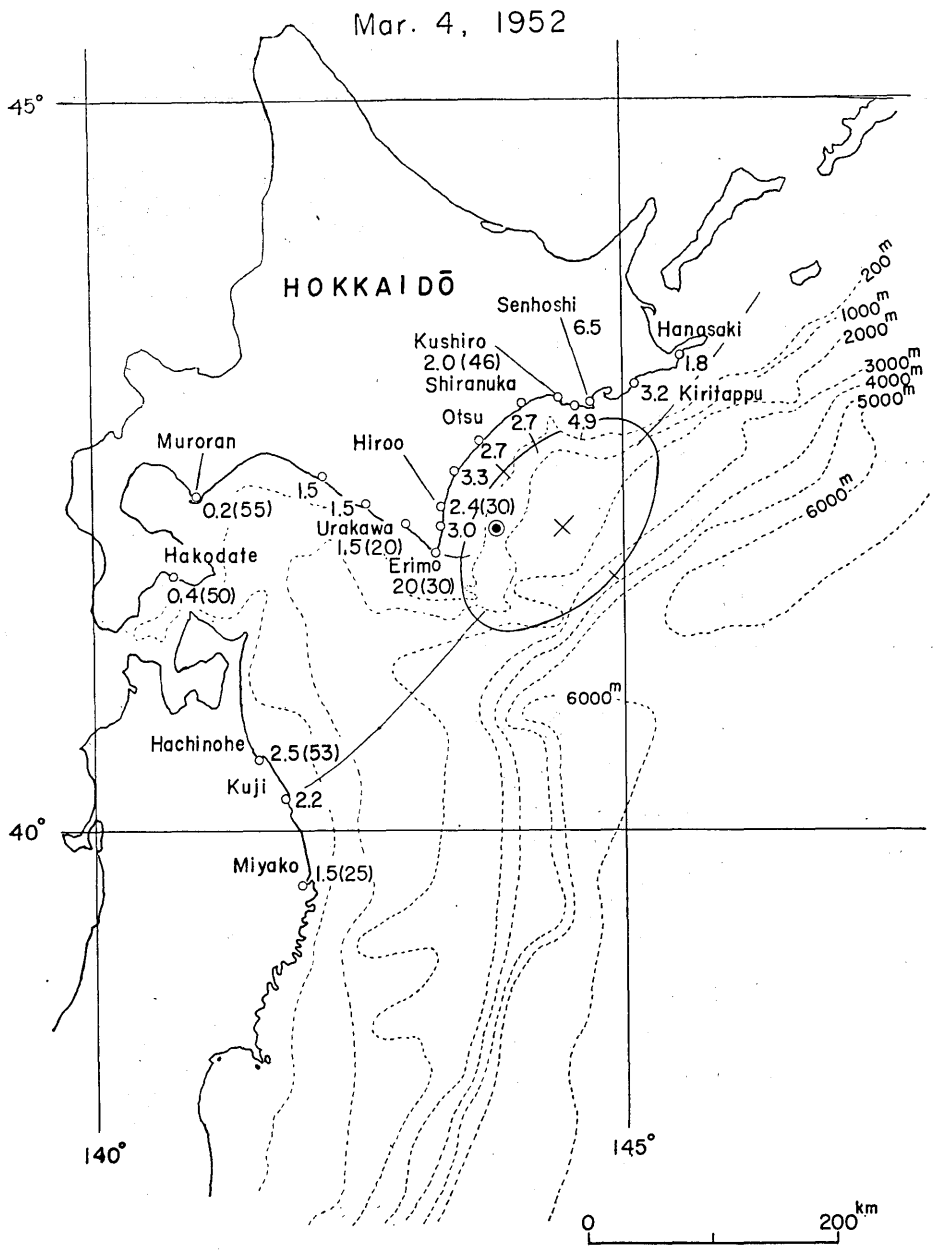

Fig. 8. The after-shock area, the distribution of inundation heights in m and periods in min, for the tsunami of Mar. 4, 1952.

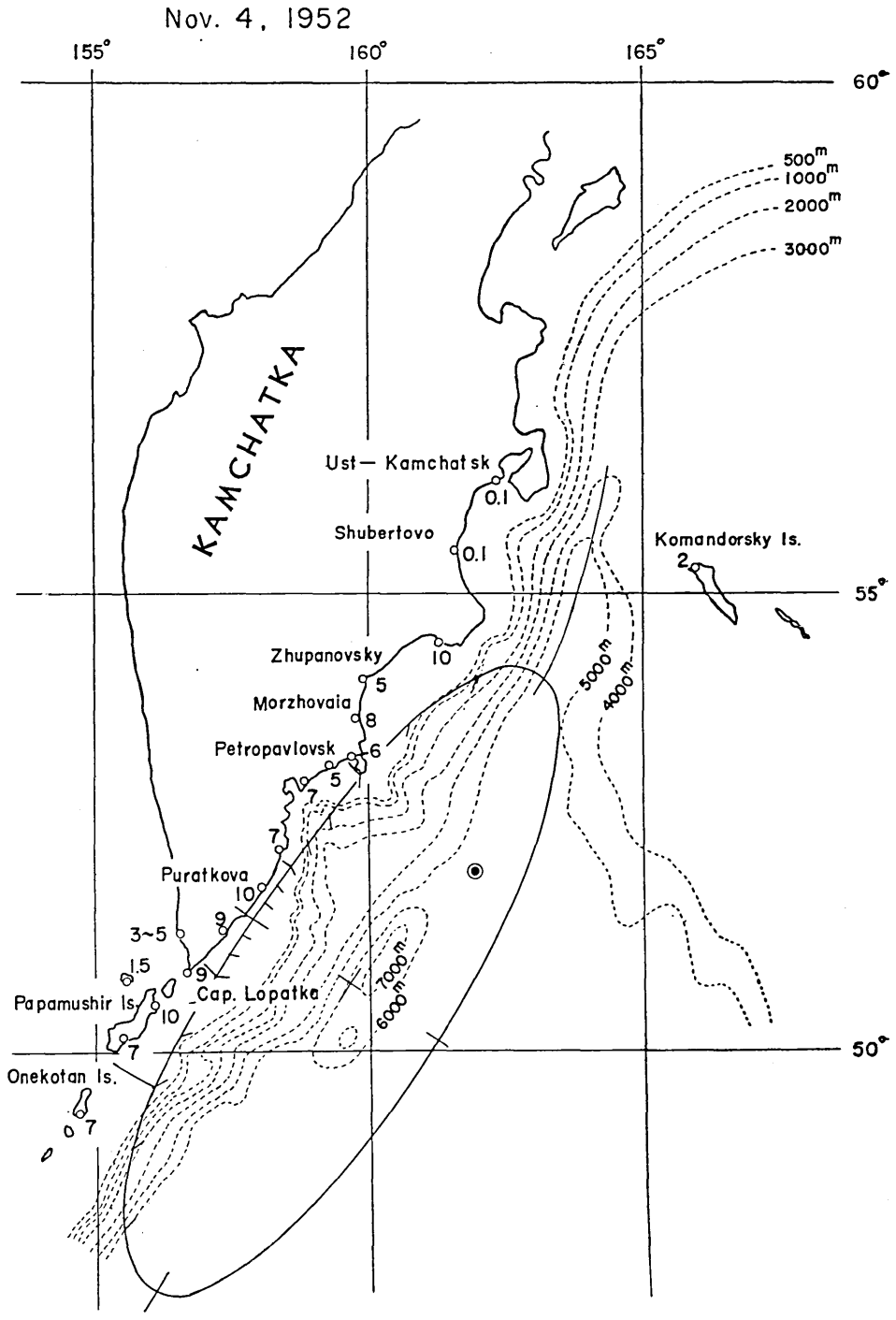

Fig. 9. The after-shock area, the distribution of inundation heights in m, for the tsunami of Nov. 4, 1952.

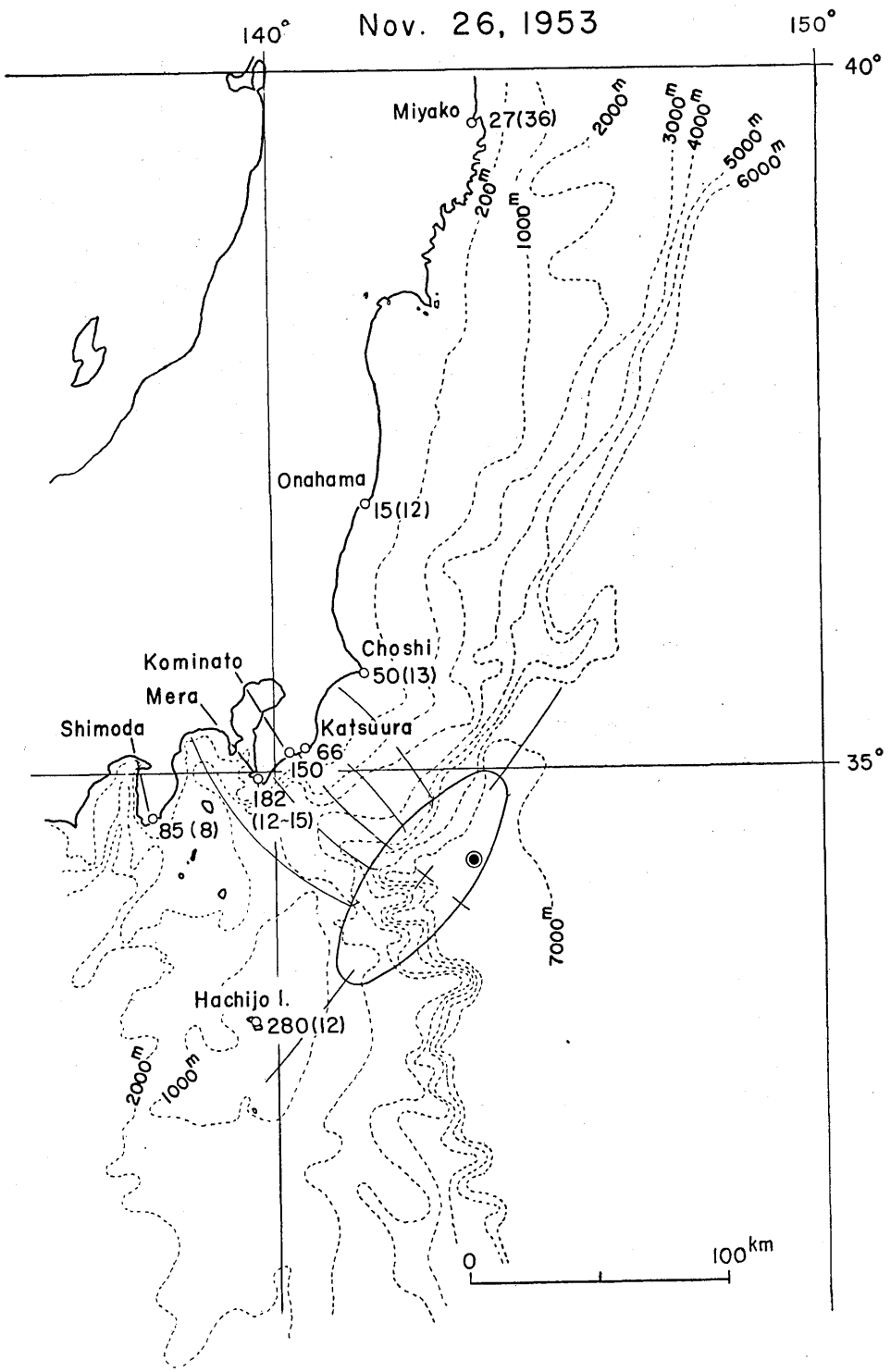

Fig. 10. The after-shock area, the distribution of wave-heights in cm and periods in min, for the tsunami of Nov. 26, 1953.

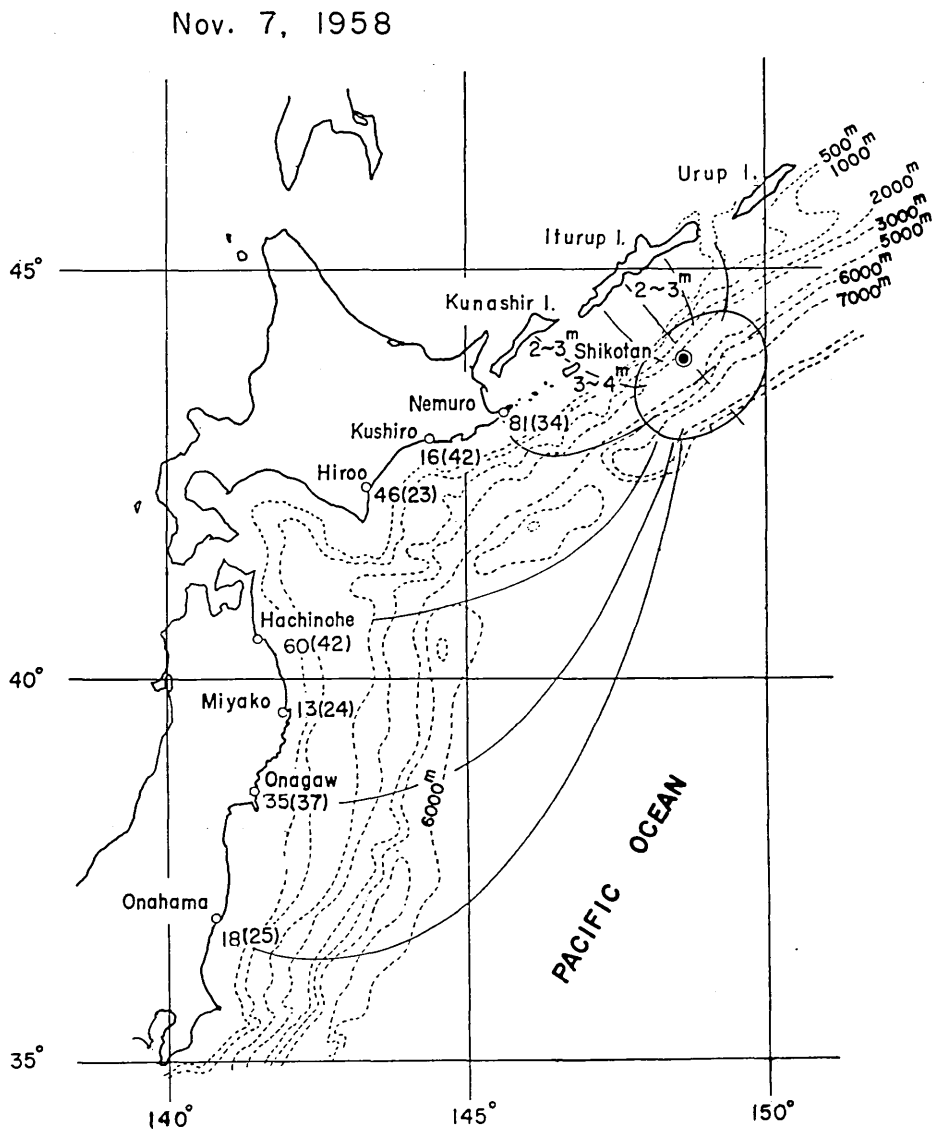

Fig. 11. The after-shock area, the distribution of inundation heights in m and periods in min, for the tsunami of Nov. 7, 1958.

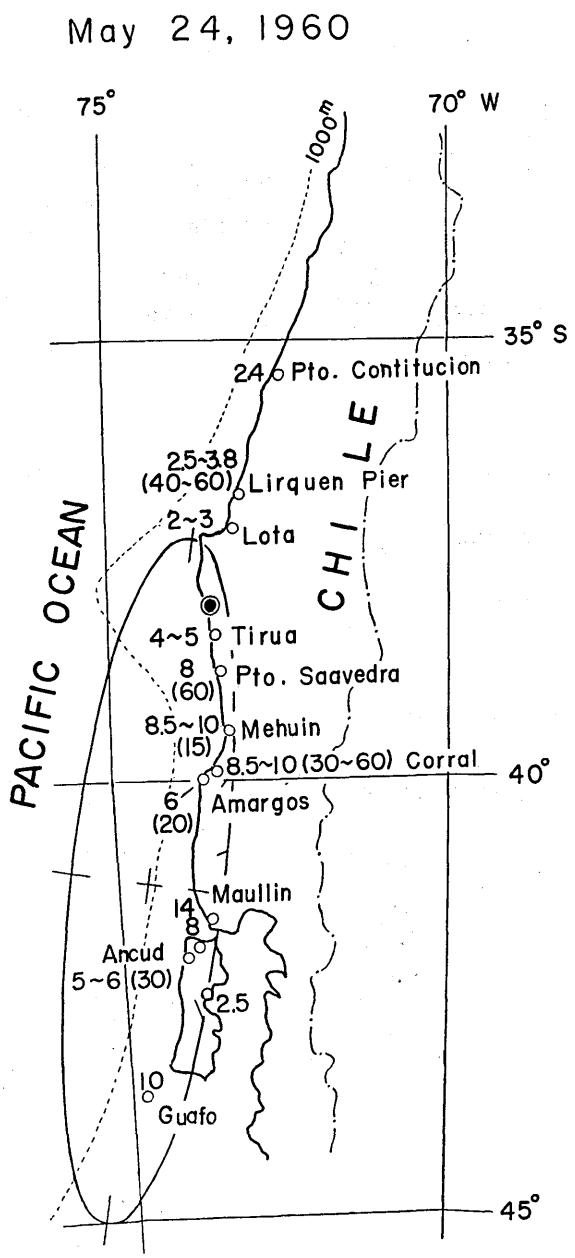

Fig. 12. The after-shock area, the distribution of inundation heights in m and periods in min, for the tsunami of May 24, 1960.

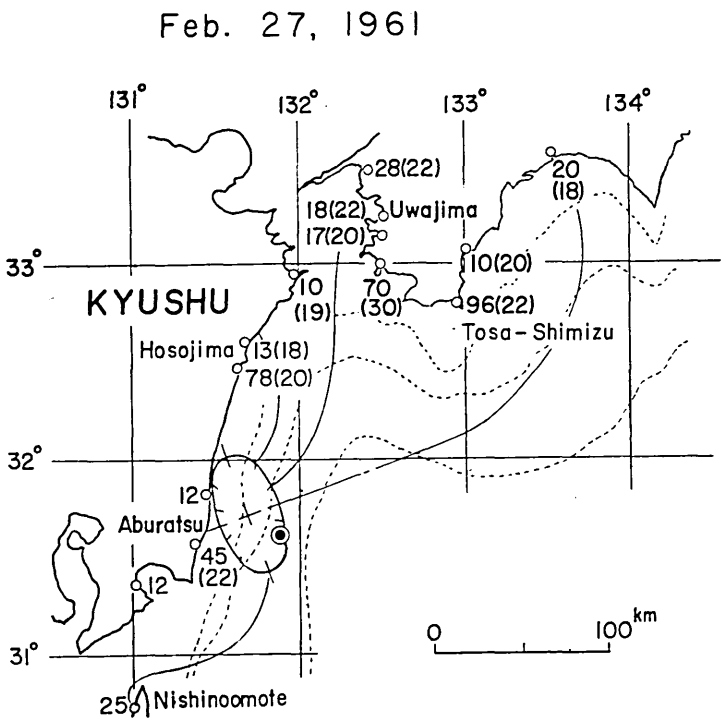

Fig. 13. The after-shock area, the distribution of wave-heights in cm and periods in min, for the tsunami of Feb. 27, 1961.

show after-shock area, the distribution of wave-heights and periods of these tsunamis. In the figures, the symbol ⊙ shows the location of the epicenter of the main shock. The epicenter seems to be located at a corner of the after-shock area.

Fig. 14 shows the variation of relative wave-heights with respect to the direction θ. θ is divided into multiples of ten degrees with the origin at the center of the after-shock area, and the angle is measured counter clockwise from the major axis as shown in Figs. 3 to 13. Tsunami waves are assumed to start from the elliptic margin of the source. Although the wave-height of a tsunami is expected to be affected by various factors, such as refraction, diffraction and reflection by the bottom irregularities, and also by the form of a bay, the wave-heights in the direction of the minor axis, as a rule, appear to be higher than those in the direction of the major axis of an after-shock area.

Fig. 15 shows the relation between the ratio of elliptic axes of an after-shock area b/a and the ratio of wave-heights H_b/H_a, where H_a is

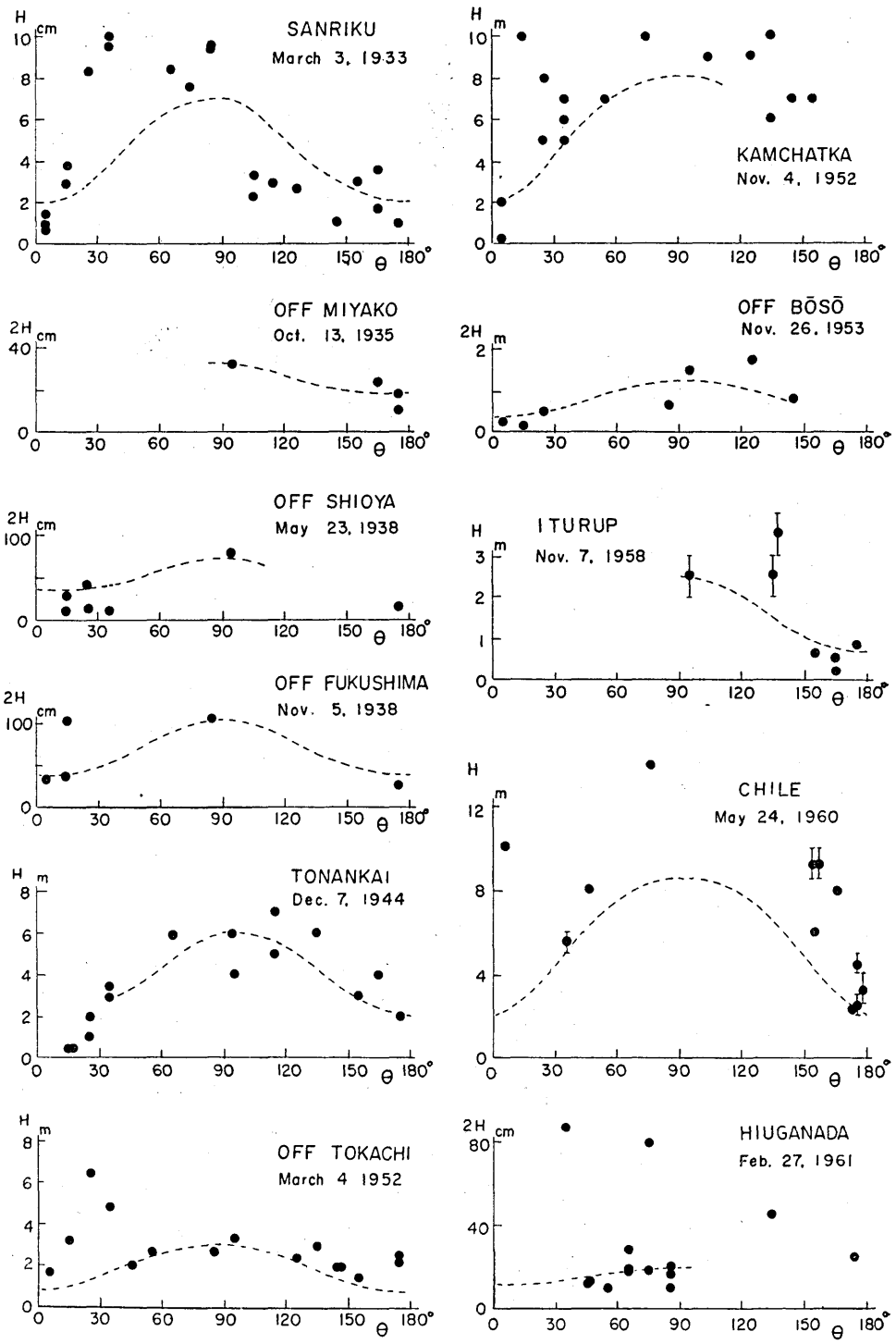

Fig. 14. The variation of relative wave-heights with respect to the direction θ.

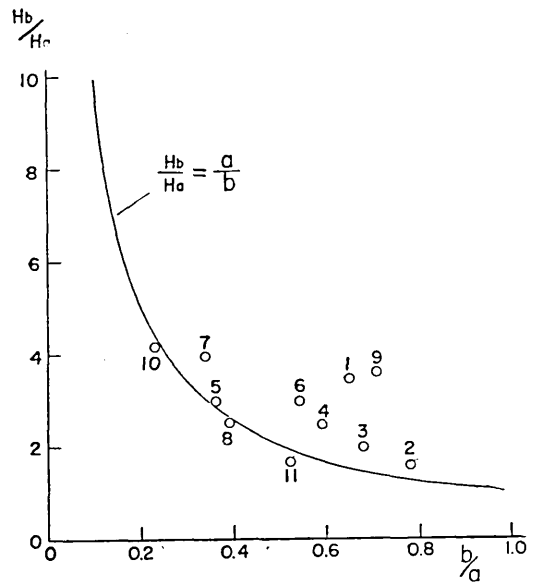

Fig. 15. The relation between the ratio of elliptic axes of an after-shock area and that of wave-heights. a: Length of the major axis at the origin.

the wave-height in the direction of the major axis and H_b is the wave-height in the direction of the minor axis of an after-shock area. The wave-height ratio seems to increase with the increase of ellipticity of the origin area. T. Momoi[10] obtained this relationship theoretically for the case of instantaneously and uniformly elevated elliptic wave origin. The formula is as follows:

$$H_b/H_a = a/b \ .$$

From a model experiment by R. Takahasi and T. Hatori[13] a similar result is also obtained for the origin with an elliptic margin, the ratio of elliptic axes being one-third. For a circular area of the after-shock, it seems that no directivity of wave-height appears. On the other hand, tsunami accompaning great earthquakes have shown a conspicuous directivity and the ratio may reach one-fourth.

5. Period

The periods of tsunami waves have been treated in a similar way. Data of period is of those observed near the coast of after-shock area. Of course, seiches in a bay excited by tsunamis have been eliminated. Fig. 16 shows the variation of relative periods with respect to the direction θ. Periods for the 1952 Kamchatka and the 1960 Chile were read from tide-gauge records on various islands of the Pacific Ocean. The direction θ at the origin is obtained from the refraction diagram. Periods at various locations are shown in Table 2.

The period T_a in the direction of the major axis of an after-shock area is longer than T_b in the direction of the minor axis as shown in Fig. 17. Although the plots of the relation between T_b/T_a and b/a are scattered as shown in Fig. 17, roughly speaking, a proportional relation-

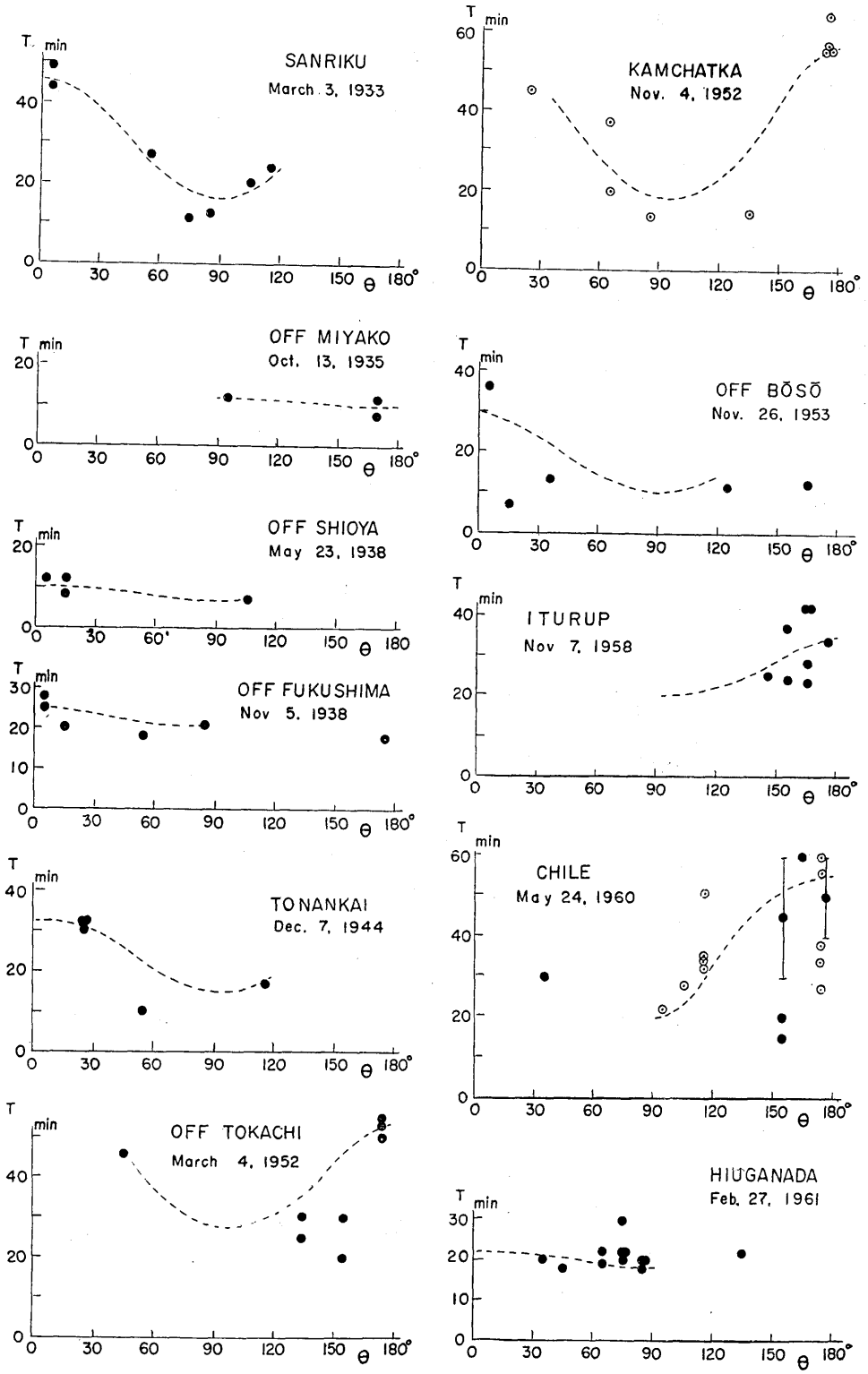

Fig. 16. The variation of relative periods with respect to the direction θ.

Table 2. Periods of tsunamis

Locality	1952 Kamchatka	Locality	1960 Chile
	min		min
Kushiro	56	Callao	60
Hachinohe	55	La Libertad	38
Onahama	55	Galapagos I.	27
Adak	45	San Lose	34
Honolulu	37	San Diago	56
Hilo	20	Honolulu	32
Midway I.	13	Hilo	34
Wake I.	14	Johnston I.	51
		Christmas I.	35
		Canton I.	28
		Pago Pago	22

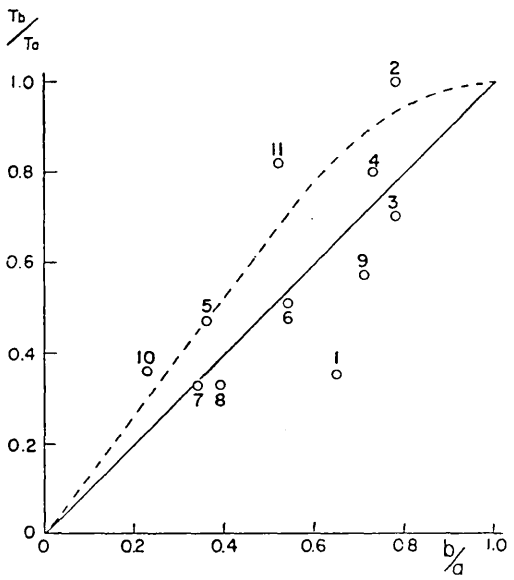

Fig. 17. The relation between the ratio of elliptic axes of an after-shock area and that of period. Broken line: Takahasi and Hatori's experiment.

ship may be discerned. In Fig. 17, the broken line indicates the value of an experiment by R. Takahasi and T. Hatori[13]. The difference in periods in the major and minor axes becomes large when an after-shock area is strongly elliptical.

6. Energy

The energy of tsunami which is originally emitted in the direction of the major or minor axes of the origin can be calculated by taking into consideration the distance from the origin. In Table 3, R_a and R_b are distances from the elliptic margin of the after-shock area in the direction of the major and minor axes respectively. Ratio of energy in both directions may be expressed as follows:

$$\frac{E_b}{E_a}=\left(\frac{H_b}{H_a}\right)^2\frac{T_b}{T_a}\frac{R_b}{R_a}\ ,$$

where the suffixes a and b indicate directions of the major and minor axes of the origin respectively. Fig. 18 shows the relationship between E_b/E_a and b/a. In this figure it seems that the directivity of energy

Table 3. Ratios of period, wave-height, distance and energy in the direction of the major and minor axes of the origin

No.	Date	T_b/T_a	H_b/H_a	R_b/R_a	E_b/E_a
1	Mar. 3, 1933	0.36	3.5	1.00	4.4
2	Oct. 13, 1935	1.00	1.6	0.16	1.6
3	May 23, 1938	0.70	2.0	0.25	0.7
4	Nov. 5, 1938	0.80	2.5	0.42	2.1
5	Dec. 7, 1944	0.47	3.0	0.50	2.1
6	Mar. 4, 1952	0.51	3.0	1.00	4.6
7	Nov. 4, 1952	0.33	4.0	1.00	5.3
8	Nov. 26, 1953	0.33	2.5	0.57	1.2
9	Nov. 7, 1958	0.57	3.6	0.30	2.2
10	May 24, 1960	0.36	4.2	1.00	6.2
11	Feb. 27, 1961	0.82	1.7	0.29	0.7

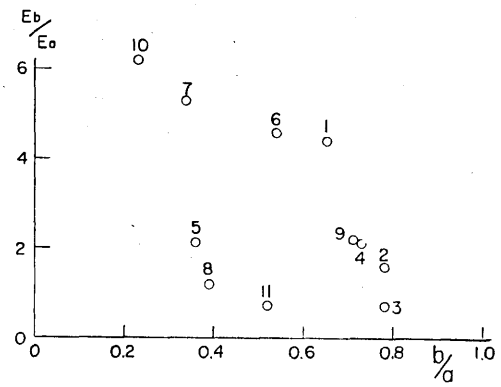

Fig. 18. The relation between the ratio of elliptic axes of an after-shock area and the ratio of energy.

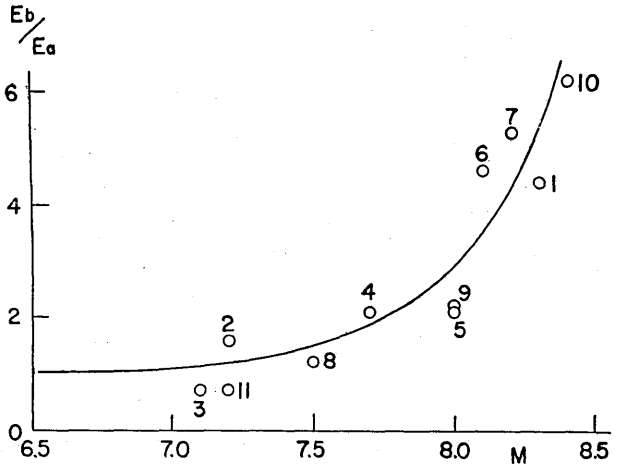

Fig. 19. The relation between the earthquake magnitude and the ratio of energy.

increases when the after-shock area becomes strongly elliptical.

Next, the relationship between the earthquake magnitude and the directivity of energy was examined. As shown in Fig. 19, directivity of energy would not appear for the earthquake magnitude 7.2 or less, but it may become two to six for the earthquake magnitude 8 to 8.3.

7. Conclusion

On the assumption that tsunami waves are generated from the after-shock area, the directivity of tsunamis has been discussed on the basis of the observed data. The form of a tsunami source in relation to an after-shock area is a question to be answered on the basis of observations to be made in the near future. The directivity of tsunamis seems to exist for a great earthquake accompanied by tsunami.

In conclusion, the author thanks Prof. R. Takahasi for his guidance and encouragement in the carrying out of this study. His thanks are also due to Assist. Prof. K. Kajiura for his valuable help and advice in the preparation of the manuscript.

---

6. 津波の方向性

地震研究所　羽 鳥 徳 太 郎

津波の方向性に関しては，これまで個々の津波につき，二，三の論文があるが，ここでは Table 1. に示す11個の津波について，津波は余震域から発生すると仮定し，余震域近傍の津波の高さおよび周期の分布 (Fig. 3～13) から津波の方向性を考察した．

余震々央の分布を包絡する領域，いわゆる余震域の形状はおよそ楕円形であり，その長径と津波の逆伝播図から求めた浪源の一次元の長さとの関係は，三陸津波を除き，およそ比例関係にある．(Fig. 1) 次に余震域の楕円軸比と津波を伴つた地震のマグニチュードとの関係は，余震々央決定の観測精度にもよるが，$b/a=-(0.13\sim0.28)M+(1.69\sim2.56)$ で表わされ，マグニチュードが小さい地震程余震域は円形で，大きくなると余震域は扁平となる．(Fig. 2)

浪源付近の沿岸で観測される津波の高さは，海底地形あるいは湾形などの影響で，かなり複雑となるが，余震域周辺から伝播する各方向の津波の高さは，余震域の短径方向が長径方向よりも大きく，(Fig. 14) マグニチュードの大きい地震程方向性がある．(Fig. 15)

津波の周期に関しても，津波の高さの場合と同様な取扱い方で，余震域の短径方向の周期が長径方向の周期より短かく，(Fig. 16) 余震域が扁平になる程，両軸方向の周期の差異が大きくなる．(Fig. 17)

次に余震域の両軸方向から伝播する津波のエネルギー比は

$$\frac{E_b}{E_a}=\left(\frac{H_b}{H_a}\right)^2\frac{T_b}{T_a}\frac{R_b}{R_a}$$

であると考え，余震域周辺から観測点までの距離 R を考慮に入れ，H は波高，T は周期で，下符付

a は余震域の長径方向，b は短径方向を表わす．これらの諸値を Table 3 に示す．この余震域の両軸方向のエネルギー比と軸比との関係は，余震域が扁平になるとエネルギーの方向性は大きくなる．(Fig. 18) またマグニチュードとの関係は Fig. 19 に示すように，津波を伴つた地震のマグニチュードが大きくなる程，エネルギーの方向性は顕著に存在するように思われる．

余震々央が内陸に広く分布する地震では，余震域と浪源との関係は不明であるが，将来観測網が充実すれば，これらの関係並びに浪源の形状も明確になることであろう．本論文では，それまでの第一段階として，上例を除いた余震域から発生する津波につき，桃井 (1962)，高橋・羽鳥 (1962) の理論およびモデル実験を考慮に入れて，津波の方向性を吟味した．